Available online at www.sciencedirect.com
SCIENCE DIRECT®
ELSEVIER
Nuclear Instruments and Methods in Physics Research B 221 (2004) 84–92
NIM B
Beam Interactions with Materials & Atoms
www.elsevier.com/locate/nimb

Experimental studies of the interaction of low energy positrons with atoms and molecules

J.P. Marler [a,*], L.D. Barnes [a], S.J. Gilbert [a], J.P. Sullivan [b], J.A. Young [a], C.M. Surko [a,*]

[a] *Department of Physics, University of California, San Diego, CA 92093-0319, USA*
[b] *Photon Factory, KEK, 1-1 Oho Tsukuba, Ibaraki 305-0801, Japan*

Abstract

This paper presents recent data on positron annihilation below and above the threshold for positronium formation in atoms and molecules. Use of a trap-based beam allows experimentation down to 50 meV and up to tens of electron volts with an energy resolution of 25 meV (FWHM). Above positronium formation, results are presented for absolute cross-section measurements in argon. Below positronium formation, absolute Z_{eff} spectrum in argon, xenon and the alkane molecules are presented. Data are compared to other experimental and theoretical results where available. The effect of fluorination of hydrocarbons on Z_{eff} below the threshold for Ps formation as well as other outstanding questions are discussed.
© 2004 Elsevier B.V. All rights reserved.

Keywords: Positron; Positron annihilation; Positronium; Z_{eff}

1. Introduction

One of the unique aspects of positron scattering, as distinguished from electron scattering, is the process of positron annihilation. Experimental and theoretical studies of direct annihilation and the process of positronium formation at higher energies are of much recent interest. In particular, since the advent of trap-based positron beams, these processes can be investigated in an energy resolved manner and with a much higher energy resolution than was previously possible [1,2]. These experimental results have encouraged new theoretical work [3–6].

A series of absolute positronium formation cross-section measurements as well as direct ionization measurements in the noble gases are in process. Preliminary results are presented in this paper. Absolute comparisons are made with other recent measurements for these cross-sections obtained using significantly different methods. While generally good agreement is found and this is encouraging, the significant differences that remain should be explored.

At incident positron energies less than the threshold for positronium formation, the unexpectedly high positron annihilation rates that are measured for molecules such as hydrocarbons have been an open question in the field for four

* Corresponding authors.
E-mail address: csurko@ucsd.edu (C.M. Surko).

0168-583X/$ - see front matter © 2004 Elsevier B.V. All rights reserved.
doi:10.1016/j.nimb.2004.03.035

decades [7–13]. This question has prompted us to pursue measurements of the annihilation parameter, Z_{eff}, resolved as a function of positron energy [14,15]. The results show large resonances associated with the vibrational motion of the molecules (i.e. vibrational Feshbach resonances) [5]. These resonances appear to be the cause of the large annihilation rates previously observed for Maxwellian distributions of positrons interacting with hydrocarbon molecules [7,11,8]. Also, the energy-resolved Z_{eff} spectra for large alkane molecules indicate the trapping of positrons into temporary bound states with these molecules.

There are still several outstanding questions concerning these resonances. The results in this paper address some of these issues including the energy position of these resonances in the alkane molecules (C_nH_{2n+2}) and the effect of certain chemical substitutions such as fluorination on Z_{eff}.

2. Experimental setup

The formation of a cold beam from a buffer gas trap is described in detail elsewhere [16]. Positrons from a radioactive source are moderated using solid neon. Using a three-stage nitrogen buffer-gas trapping scheme, positrons are loaded into a Penning–Malmberg trap and cooled to the wall temperature (300 K). The accumulated positrons are then electrostatically forced out of the trap as a pulsed, magnetically guided beam of energy width $\sim$25 meV (FWHM). The experiments described here use pulses of $\sim 5\times 10^4$ positrons at a repetition rate of 3 Hz.

2.1. Ps formation and ionization

For the positronium formation and ionization experiments, the positron beam is magnetically guided through a cell containing the test gas at pressures from 0.05 to 0.5 mTorr. Since the scattering takes place in a strong magnetic field, it is helpful to consider the total energy of the positrons as separated into its two components, a parallel component (energy of the motion along the magnetic field lines) and a perpendicular component (energy in the cyclotron motion in the plane perpendicular to the magnetic field).

Positrons that have not annihilated in the gas cell continue down the beam line passing through a retarding potential analyzer (RPA) which is used to analyze the parallel energies of the positrons. Positrons that have enough parallel energy to pass through the RPA annihilate on a plate at the end of the vacuum chamber, and the annihilation gamma rays are detected by a NaI crystal [17].

To measure positronium formation cross-sections, the RPA is kept at zero volts. The signal strength, I_0, when the positrons do not have enough energy to form positronium is compared to the signal strength at higher energies, $I_{\text{Ps}}(\varepsilon)$. The test gas pressure for these experiments is chosen to limit scattering to less than 15%. The positronium formation cross-section is then given by

$$\sigma_{\text{Ps}}(\varepsilon) = \frac{1}{n_{\text{m}} l}\frac{I_0 - I_{\text{Ps}}(\varepsilon)}{I_0}, \tag{1}$$

where n_{m}, the target number density, and l, the effective path length, can be measured. Using this technique, absolute cross-section measurements can be made without the need for normalization to other measurements.

In order to measure direct ionization cross-sections, the experiment takes advantage of the ability to vary the magnetic field between the scattering and the analyzing regions. In a slowly varying magnetic field the ratio of the perpendicular component of energy to the magnetic field strength, $E_\perp/B$, remains constant. This is crucial because the positrons can undergo both elastic and inelastic scattering in the gas cell. These processes can change both the total positron energy and shift some of the energy from parallel motion into perpendicular (i.e. cyclotron) motion. Reducing the magnetic field in the analyzing region redirects the perpendicular energy back into the parallel direction. Although angular information is lost, the integral cross-sections for inelastic processes can be determined since the analyzer now measures the total final energy of the positrons.

For ionization, the RPA is set to the transport energy of the positrons (i.e. the energy of the positrons as they leave the trap) minus the ionization

energy of the atom or molecule. Therefore only positrons that have lost less than the ionization energy will pass through the RPA and be detected. Denoting the transmitted signal strength as $I_{\mathrm{Ion}}(\varepsilon)$, the absolute direct ionization cross-section is given by

$$\sigma_{\mathrm{Ion}}(\varepsilon) = \frac{1}{n_{\mathrm{m}} l} \frac{I_{\mathrm{Ps}}(\varepsilon) - I_{\mathrm{Ion}}(\varepsilon)}{I_0}. \quad (2)$$

2.2. Annihilation below Ps formation

In order to measure annihilation below Ps formation, the pulses of positrons are magnetically guided into an electrode filled with the gas to be studied at pressures ranging from 1 mTorr to 0.1 μTorr. The bias on this electrode sets the energy of the positrons in the region containing the sample gas. The positron energy can be varied from 50 meV upward. Single annihilation events are detected by a CsI crystal and accompanying photodiode just outside the vacuum chamber. Using the measured number of positrons per pulse, the length of the gas-filled region and the detector efficiency, we obtain the annihilation cross-section, σ. The normalized annihilation rate, Z_{eff}, can then be calculated using

$$Z_{\mathrm{eff}} = \frac{\sigma v}{\pi r_0^2 c}, \quad (3)$$

where v is the velocity of the positron, r_0 is the classical electron radius and c is the speed of light [15]. The total number of annihilation events is typically 1 event per 10^4 positrons dumped of which we detect on the order of 1%.

3. Results

3.1. Ps formation and ionization

Positrons can ionize atoms and molecules by three processes: direct ionization,

$$A + \mathrm{e}^+ \rightarrow A^+ + \mathrm{e}^+ + \mathrm{e}^- \quad (4)$$

positronium formation,

$$A + \mathrm{e}^+ \rightarrow A^+ + \mathrm{Ps} \quad (5)$$

and direct annihilation, which is predominantly 2γ decay,

$$A + \mathrm{e}^+ \rightarrow A^+ + 2\gamma \quad (6)$$

The experiments described here can distinguish these processes because positronium formation and direct annihilation result in a loss of positrons from the beam. Direct ionization is an inelastic process and leaves positrons in the beam with a kinetic energy reduced by at least the ionization energy of the atom.

The first two processes have cross-sections $\sim a_0^2$, whereas the latter has a much smaller cross-section ($\sigma = \pi r_0^2 c Z_{\mathrm{eff}}/v \ll a_0^2$). At energies higher than the threshold for positronium formation, direct annihilation cannot be distinguished from Ps formation, but the contribution from the former is expected to be small. Direct annihilation can be measured for energies less than the threshold for Ps formation since Ps formation is forbidden in this regime.

Fig. 1 shows the current data for positronium formation in argon compared to other recent experimental and theoretical work. The first calculation was done using a static-exchange approximation to calculate positronium formation in the ground state [20]. Also shown in the figure are the predictions of a more recent calculation (scaled by 0.5) that uses the distorted-wave Born

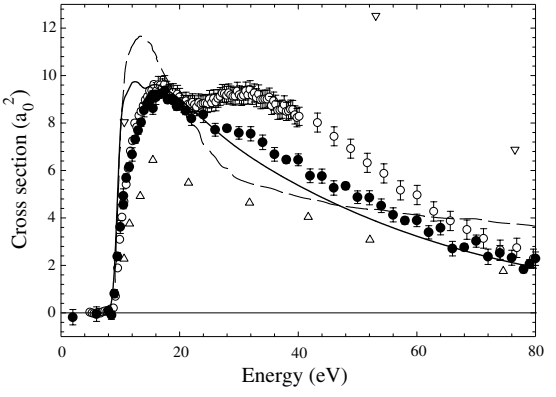

Fig. 1. Positronium formation cross-section for positron impact on argon: (●) present data; (○) data from [18]; (△, ▽) lower and upper experimental limits from [19]; (– –) theory of [20]; (–) updated theory of [21] scaled by ×0.5.

approximation and includes both ground-state and excited-state Ps formation [21].

Also plotted are the other most recent experimental measurements (open circles). The two experimental techniques are quite different so a brief explanation of the previous work by Laricchia et al. is in order. Total ionization cross-sections were measured by collecting ions in a crossed beam experiment [18]. Previously, the direct ionization cross-section at these energies was measured by counting the ions formed in a crossed beam arrangement in coincidence with positrons that had lost the ionization energy or greater [22]. Both of these sets of measurements were normalized to the analogous electron cross-sections at high energies. Since direct ionization and positronium formation are by far the biggest contributors to the total ionization cross-section at these energies, the positronium formation cross-section was then determined as the difference of the above two normalized cross-sections [18].

Considering the difference in the experimental methods, the generally good, quantitative agreement between the measurements shown in Fig. 1 is encouraging. However, it is interesting to note the differences between the cross-sections. Specifically at incoming positron energies in the range between 20 and 60 eV, the Ps formation cross-sections of [18] are higher and exhibit a second peak nearly equal in height to the one at threshold.

The current method determines Ps formation cross-sections by directly measuring total positron loss. This is in contrast to the method of [18] which calculates Ps formation cross-section by taking the difference of the total ionization cross-section and the direct ionization cross-section. Thus one explanation of the discrepancies between the two sets of measurements illustrated in Fig. 1 would be a relatively small undercounting of direct ionization events in previous measurements (i.e. done by coincidence measurements of positrons and positive ions).

As we recently conducted measurements of the direct ionization of argon from threshold to 80 eV, we found it of interest to calculate the positronium formation cross-section using the method of [18] but incorporating our new direct ionization cross-section measurements. Shown again in Fig. 2 are

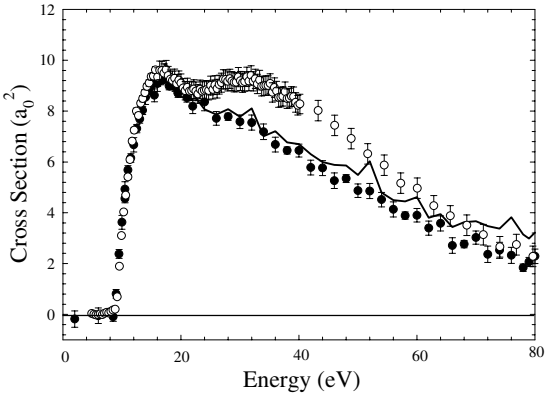

Fig. 2. Positronium formation cross-section for positron impact on argon (●) present data; (○) data from [18]; (–) Ps formation calculated by taking the difference between the total ionization cross-section from [18] and current direct ionization measurements from the present work.

the current Ps formation measurements and those of Laricchia et al. [18]. The solid line gives the Ps formation cross-section calculated by subtracting our measured direct ionization cross-section from the total ionization cross-section reported in [18]. We note that this results in noticeably better agreement with the current Ps formation data which does not rely on a measured ionization cross-section.

We have measured the Ps formation and direct ionization cross-sections in Kr and also made similar comparisons with the measurements of [18]. As in the case of argon, small discrepancies between our Ps formation data and that reported by Laricchia et al. are significantly reduced if we replace the direct ionization measurements of Laricchia et al. with our own in the calculation of the Ps formation cross-section.

3.2. Annihilation below Ps formation

The behavior of Z_{eff} just below the threshold for positronium formation has been a subject of some debate [12,23,24]. Fig. 3 shows the energy-resolved Z_{eff} spectrum for xenon and argon. Comparison to calculations by Mitroy and Ivanov [25] show good agreement with no fitted parameters. For the targets we have examined to date, argon, xenon and butane (C_4H_{10}), we see no increase in Z_{eff} for

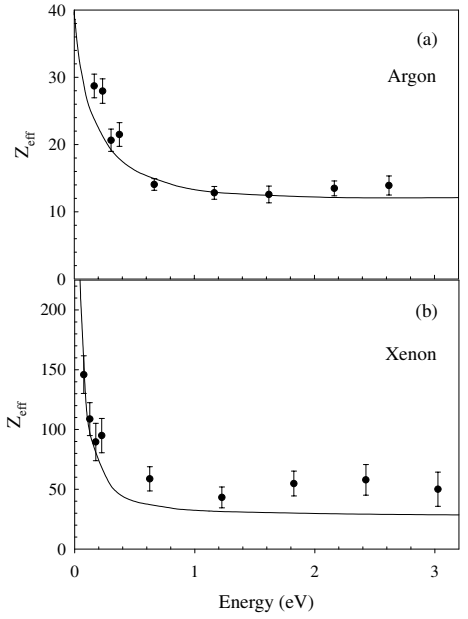

Fig. 3. The annihilation parameter, Z_{eff}, for argon (a) and xenon (b) as a function of incident positron energy. The solid lines are the results of a calculation by Mitroy and Ivanov [25] with no fitted parameters. The threshold for positronium formation is 7.2 eV for argon and 5.33 eV for xenon.

values of positron energy from 0.5 eV to within an electron volt or two of the positronium threshold. The Z_{eff} spectrum in this region is flat, as is shown in Fig. 3 for argon and xenon. Investigating the region very close to the Ps threshold is more difficult due to small numbers of positrons with energies larger than the beam energy which fall above the threshold for positronium formation. Measurements at higher energies may also be skewed by the presence of trace elements in the vacuum system which have a Ps threshold lower than that of the test gas. Because of these difficulties, we have not investigated the region very close to the Ps formation threshold. To date, we have seen no appreciable increase in Z_{eff} as positron energy approaches the positronium threshold.

The main focus of our annihilation experiments has been understanding the large rates observed in a variety of molecules, with alkanes (C_nH_{2n+2}) being a prototypical example. Several of the figures included here for alkanes can be found in [14] and [15]. Fig. 4 shows Z_{eff} for propane (C_3H_8) as a

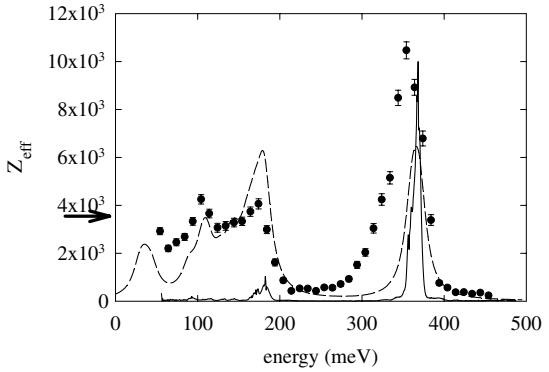

Fig. 4. The annihilation parameter, Z_{eff}, for propane (C_3H_8) (●) as a function of incident positron energy [15]. For comparison, the dashed line shows the fundamental vibrational modes plotted as Lorentzian lineshapes of width of 10 meV and arbitrary height. The solid line is the IR absorption spectrum (scaling arbitrary).

function of incident positron energy. The most striking feature of the Z_{eff} spectrum for these alkanes is the occurrence of large resonance peaks in the energy region of the molecular vibrations (i.e. $\leqslant 500$ meV). Comparison to the fundamental vibrational modes of these molecules (see Fig. 4) shows that the resonances in Z_{eff} appear lower than the energies of the vibrational modes by $\sim$15 meV.

According to Gribakin, such enhancements of Z_{eff} can be attributed to vibrational Feshbach resonances (VFR). Here, we briefly describe this model which is discussed in more detail elsewhere [24]. If the positron-molecule interaction is sufficiently attractive to support a positron-molecule bound state, this bound state can be populated by positrons which give up energy by vibrationally exciting the target molecule. These states are temporary, since the vibrational energy of the molecule can also be used to eject the positron from the bound state back into the continuum. Nonetheless, positrons in the temporary bound state have much larger overlap with the molecular electrons than do free positrons, and this results in an enhancement of Z_{eff}.

This resonant enhancement in annihilation should occur when the energy of the free positron plus that of the target molecule in its vibrational ground state is close to the energy of the bound positron-molecule system with the molecule

vibrationally excited. Assuming the single vibrational excitation affects the positron-molecule interaction very little, the condition on the incident positron energy, ε_i, is

$$\varepsilon_i + E_0 = \varepsilon_b + E_{ex}, \tag{7}$$

where E_0 and E_{ex} are the ground and vibrationally excited molecular energies and ε_i and ε_b are the energies of the positron in the incident continuum state and the temporary bound state.

Since ε_b is assumed to be less than zero for a Feshbach resonance, the enhancement of the annihilation rate is expected to occur for positrons with energy less than the energies of the vibrational modes by ε_b. This can be seen in Fig. 5, which compares the Z_{eff} spectrum for hexane (C_6H_{14}), nonane (C_9H_{20}), and dodecane ($C_{12}H_{26}$). It is apparent that, for these alkanes, the maximum of the large peak, which is associated with the C–H stretch vibrational mode, appears at decreasing energies as the molecular size increases. In the context of the VFR model, this is interpreted as increasing positron-molecule binding energy, $-\varepsilon_b$.

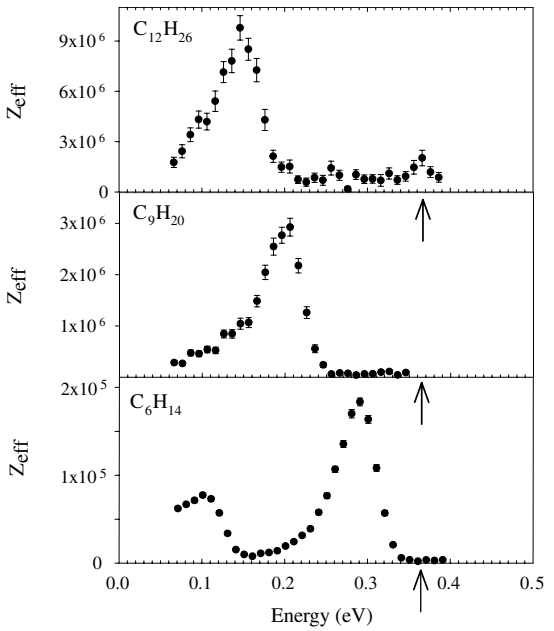

Fig. 5. Z_{eff} for hexane (C_6H_{14}) nonane (C_9H_{20}), and dodecane ($C_{12}H_{26}$). The arrows on the abscissa indicate the energy of the C–H stretch vibrational modes. See [15].

It should also be noted that not only is the C–H stretch peak shifted, but the entire Z_{eff} spectrum is shifted downward in energy by approximately the same amount. This is to be expected if the binding of a positron to the molecule depends only weakly on the specific vibration excited.

Similar studies of the deuterium-substituted equivalents of some of the alkanes confirm the dependence of these resonances on the vibrational energies of the molecules. The energy resolved Z_{eff} data, such as that shown in Figs. 4 and 5, and their interpretation in terms of vibrational Feshbach resonances provide the most direct evidence to date that positrons bind to molecules.

3.3. Annihilation in fluorine substituted alkane molecules

The effect of chemical substitution on the Z_{eff} spectra of molecules is not well understood. Fig. 6 compares the Z_{eff} spectrum for two alkanes to

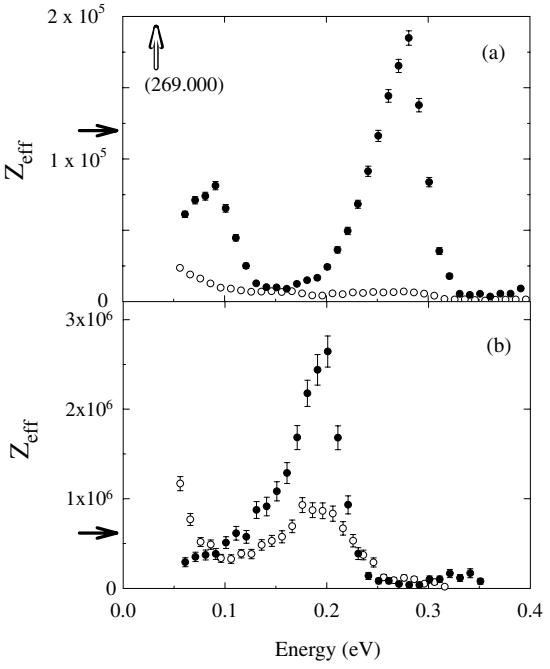

Fig. 6. (a) Z_{eff} for hexane (C_6H_{14}) (●) and 1-fluorohexane ($C_6H_{13}F$) (○). (b) Z_{eff} for nonane (C_9H_{20}) (●), and 1-fluorononane ($C_9H_{19}F$) (○) [15]. The solid and open arrows indicate Z_{eff} for a Maxwellian distribution of positrons at 300 K.

those of their singly fluorinated equivalents. In both cases, the effect of the fluorination is a marked decrease in the strength of the resonance associated with the C–H stretch vibrational mode and an enhancement of Z_{eff} at lower energies. In the case of 1-fluorohexane, this low-energy enhancement is seen in the increased Z_{eff} for thermal distributions of positrons (open arrow). For 1-fluorononane, the low-energy enhancement is also visible in the energy-resolved spectrum.

Another observation from this comparison is that, for the fluorinated molecules, the C–H stretch peak, although significantly reduced in magnitude, appears at approximately the same energy as in the fully hydrogenated molecules. We interpret this to mean that the positron binding energy is not significantly changed with the addition of a single fluorine.

In smaller molecules, fluorine substitution has another effect on Z_{eff} that requires further scrutiny. Fig. 7 compares the Z_{eff} spectra of methane (CH_4), methyl fluoride (CH_3F), difluoromethane (CH_2F_2), trifluoromethane (CHF_3) and carbon tetrafluoride (CF_4). For methane and the fully fluorinated carbon tetrafluoride (CF_4), no peaks are observed although there are several available vibrational modes that could give rise to peaks in Z_{eff}. As the first fluorine is substituted (CH_3F), a pronounced resonance appears near 150 meV. This mode persists but decreases in magnitude as more fluorine atoms are substituted.

Comparison with the values of Z_{eff} for thermal distributions of positrons (shown as arrows on the y-axis), reveals that the annihilation rate at lower energies is much larger than Z_{eff} in the range of the energy-resolved data. This is observed for all of the molecules except CF_4. One explanation of such low energy enhancement of Z_{eff} [5] proposes that either low-lying virtual states or weakly-bound positron-molecule states could produce a Z_{eff} spectrum of the form

$$Z_{\text{eff}}(E) = \frac{A}{E + |E_0|} + C. \tag{8}$$

Here E is the incident positron energy, E_0 is the energy of the low-lying virtual state or bound state and A is a constant independent of positron energy. The constant, C, represents an energy-independent contribution due to other processes. Fig. 8 shows the Z_{eff} spectra for methane and carbon tetrafluoride compared with fits of the form of Eq. (8) shown as the solid curves. The constants, A, were determined by requiring the curve to be consistent with the previously-measured [11] values of Z_{eff} for a Maxwellian distribution of positrons at room temperature (i.e. 142 for methane and 54.4 for carbon tetrafluoride). The constant, C, was determined from the measured values of Z_{eff} for energies greater than 1 V where the contribution of the first term in Eq. (8) is small. The energy of the virtual or bound state is then the

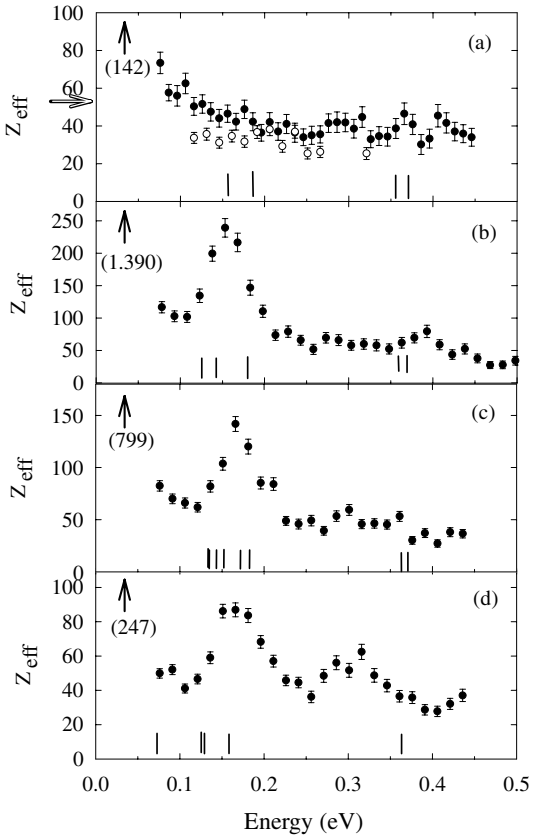

Fig. 7. Positron annihilation rates, Z_{eff}, for (a) methane (CH_4) and carbon tetrafluoride (CF_4), solid and open circles, respectively, (b) methyl fluoride (CH_3F) (c) difluoromethane (CH_2F_2) and (d) trifluoromethane (CHF_3) [15]. Vertical lines indicate the energies of the vibrational modes. Arrows indicate Z_{eff} for a thermal distribution of positrons. In graph (a) the solid arrow refers to methane and the open arrow to carbon tetrafluoride.

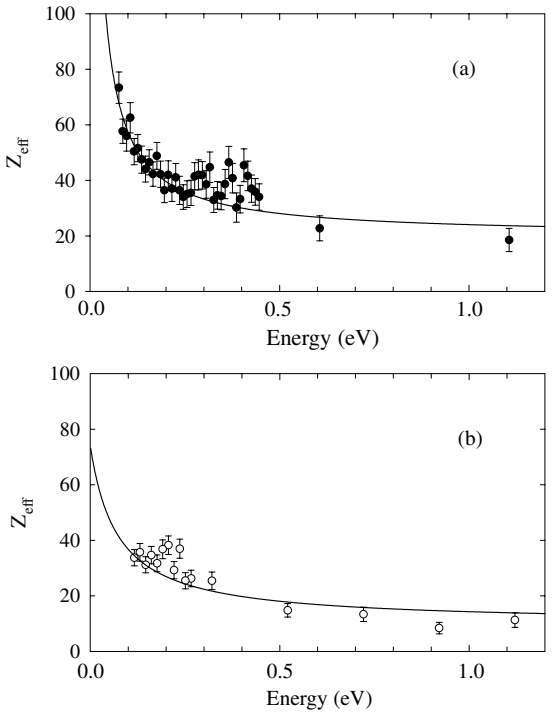

Fig. 8. (a) Z_{eff} for methane (CH_4) (b) and carbon tetrafluoride (CF_4). The solid lines are a best fit (squared difference) of the form given by Eq. (8) with a single fit parameter, E_0.

only fit parameter. The best fits to the data give the energy of the virtual or bound state as ±10 mV for methane and ±72 mV for carbon tetrafluoride. The constants A are 4.1 and 4.6 for CH_4 and CF_4, respectively. These values of $|E_0|$ are within a factor of 2–3 agreement with a similar estimate (also based on Eq. (8)) for these molecules made by Gribakin [5] using only the 300 K values of Z_{eff}. The sign of E_0 cannot be determined since, by Eq. (8), a bound state and virtual state have the same effect on Z_{eff}.

4. Concluding remarks

This paper presents new results in annihilation experiments both below and above the threshold for positronium formation. Above the Ps formation threshold, absolute comparison with other recent experiments confirms the general magnitude of the cross-sections which we hope will encourage further theoretical interest. In addition, specific differences noted between the experimental results suggest that future study is warranted.

Below the Ps threshold, results are presented that explain the anomalously high Z_{eff} values first seen in experiments done with thermal distributions of positrons over 40 years ago in terms of vibrational Feshbach resonances. The data provide evidence that positrons bind to hydrocarbon molecules. However, these new experimental results still leave many unanswered questions. The data presented here highlight the unexplained changes in the Z_{eff} spectra due to the addition of a fluorine atom to either large or small alkane molecules.

We also wish to stress the power of a trap-based cold positron beam to make absolute, energy resolved scattering measurements and measurements of Z_{eff} with excellent resolution. We encourage future theoretical work in this area and are open to suggestions of molecules that may be studied experimentally and for which Z_{eff} could be calculated.

Acknowledgements

The authors would like to thank E.A. Jerzewski for his expert technical assistance. We would also like to acknowledge helpful discussions with G.F. Gribakin, James Walters and G. Laricchia and thank them for providing tabulated results before publication. This work is supported by the National Science Foundation, grant PHY 98-76894 and the Office of Naval Research, grant N00014-02-1-0123.

References

[1] S.J. Gilbert, C. Kurz, R.G. Greaves, C.M. Surko, Appl. Phys. Lett. 70 (1997) 1944.
[2] S.J. Gilbert, R.G. Greaves, C.M. Surko, Phys. Rev. Lett. 82 (1999) 5032.
[3] See articles in Can. J. Phys. 76 (1996) 313.
[4] M. Kimura, M. Takeawa, Y. Itikawa, H. Takaki, O. Sueoka, Phys. Rev. Lett. 80 (1998) 3936.
[5] G.F. Gribakin, Phys. Rev. A A61 (2000) 022720.

[6] F.A. Gianturco, T. Mukherjee, Eur. Phys. J. D 7 (1999) 211.
[7] D.A.L. Paul, L. Saint-Pierre, Phys. Rev. Lett. 11 (1963) 493.
[8] G.R. Heyland, M. Charlton, T.C. Griffith, G.L. Wright, Can. J. Phys. 60 (1982) 503.
[9] C.M. Surko, A. Passner, M. Leventhal, F.J. Wysocki, Phys. Rev. Lett. 61 (1988) 1831.
[10] T.J. Murphy, C.M. Surko, Phys. Rev. Lett. 67 (1991) 2954.
[11] K. Iwata, R.G. Greaves, T.J. Murphy, M.D. Tinkle, C.M. Surko, Phys. Rev. A 51 (1995) 473.
[12] G. Laricchia, C. Wilkin, Phys. Rev. Lett. 79 (1997) 2241.
[13] E.P. da Silva, J.S.E. Germane, M.A.P. Lima, Phys. Rev. Lett. 77 (1996) 1028.
[14] S.J. Gilbert, L.D. Barnes, J.P. Sullivan, C.M. Surko, Phys. Rev. Lett. 88 (2002) 043201.
[15] L.D. Barnes, S.J. Gilbert, C.M. Surko, Phys. Rev. A 67 (2003) 032706.
[16] S.J. Gilbert, J.P. Sullivan, R.G. Greaves, C.M. Surko, Nucl. Instr. and Meth. B 171 (2000) 81.
[17] J.P. Sullivan, S.J. Gilbert, J.P. Marler, R.G. Greaves, S.J. Buckman, C.M. Surko, Phys. Rev. A 66 (2002) 042708.
[18] G. Laricchia, P.V. Reeth, M. Szłuińska, J. Moxom, J. Phys. B 35 (2002) 2525.
[19] T.S. Stein, W.E. Kauppila, C.K. Kwan, S.P. Parik, S. Zhou, Hyperfine Interact. 73 (1992) 53.
[20] M.T. McAlinden, H.R.J. Walters, Hyperfine Interact. 73 (1992) 65.
[21] S. Gilmore, M. T. McAlinden, H.R.J. Walters, private communication, 2003.
[22] V. Kara, K. Paludan, J. Moxom, P. Ashley, G. Laricchia, J. Phys. B 30 (1997) 3933.
[23] G. Laricchia, C. Wilkin, Nucl. Instr. and Meth. B 143 (1998) 135.
[24] G.F. Gribakin, J. Ludlow, Phys. Rev. Lett. 88 (2002) 163202/1-4.
[25] J. Mitroy, I.A. Ivanov, Phys. Rev. A 65 (2002) 042705.